Electron energy relaxation via LO-phonon emission in free standing GaAs wafers

1990 J. Phys.: Condens. Matter 2 7465

(http://iopscience.iop.org/0953-8984/2/36/009)

J. Phys.: Condens. Matter 2 (1990) 7465–7471. Printed in the UK

Electron energy relaxation via LO-phonon emission in free-standing GaAs wafers

N C Constantinou and B K Ridley
Department of Physics, University of Essex, Colchester CO4 3SQ, UK

Received 30 March 1990, in final form 8 June 1990

Abstract. The electron LO-phonon scattering rate is obtained for a thin free-standing GaAs wafer. The carriers are assumed to occupy only the lowest subband. The choice of confining potential is shown to make a quantitative difference in the variation of the scattering rate with wafer thickness. Phonon confinement effects are demonstrated to manifest themselves for thicknesses less than around 500 Å. It is shown that purely longitudinal surface modes are not allowed in these free-standing structures. Surface electromagnetic waves (polaritons), which *are* normal modes of the system exist, though it is argued that their interaction with electrons ought to be weak.

1. Introduction

In low-dimensional semiconductor structures such as the GaAs/AlGaAs system, the interaction of electrons with the polar LO-phonons is of fundamental importance for high field transport. Early theoretical calculations assumed the bulk phonon approximation [1–3]. This was subsequently relaxed in view of light-scattering measurements indicating confinement of the optical modes in the GaAs layer [4]. Various theoretical models have been proposed to describe these confined phonons. The most commonly used are the dielectric continuum theory [5, 6] and the dispersive Born and Huang model [7–9]. Both predict guided and interface modes for the GaAs/AlGaAs system although the mode potential symmetries are at variance. What experimental evidence exists suggests that it is the dispersive Born and Huang theory which correctly describes the symmetry associated with the potentials [10]. Nevertheless, both descriptions agree that interface modes play a dominant role in electron energy relaxation in these GaAs/AlGaAs structures, especially for thin slabs [9]. As for a free-standing GaAs wafer we demonstrate that LO-interface modes do not exist and hence cannot relax the carrier energy at high temperatures.

In this paper we consider the interaction of electrons with the LO-phonons associated with free-standing GaAs wafers. Indeed, free-standing GaAs wires have recently been fabricated by Hasko *et al* [11] and work is under way to grow thin free-standing wafers [12]. The electrons in these structures are in general confined to a volume different from that of the slab. In practice the carriers deplete away from the surface due to the pinning of the Fermi level by surface states [11]. Experimentally, the confinement region may be controlled by gating the device or varying the doping density. Often in transport studies it is advantageous for the width of the electron gas to be narrow in order to

0953-8984/90/367465 + 07 $03.50

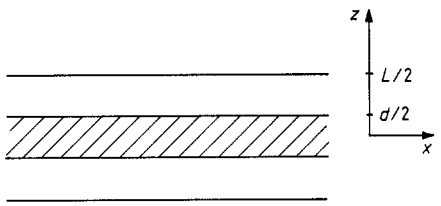

Figure 1. The free-standing GaAs wafer of width L. The hatched area illustrates the Q2D electron gas of thickness d. Also depicted is the coordinate system employed.

minimise intersubband events (the so-called extreme quantum limit). The relationship between this width and the various parameters (wafer width, doping density, gate voltage) is complex and we do not dwell on it here.

Figure 1 illustrates the system which we consider; a free-standing slab of thickness L with the quasi-two-dimensional (Q2D) electron gas confined to a layer of thickness d. The confining potential will in practice be approximately quadratic. It is one of the aims of this paper to compare the predictions assuming the often used infinite confining potential for the scattering rate with that obtained with a more realistic potential. Another question that needs to be addressed is how thick the wafer should be in order that phonon confinement effects are noticeable. We will see that for typical carrier energies the width of the GaAs slab should be less than about 500 Å.

Earlier work on this system has been carried out and our results are compared where appropriate.

2. The interaction Hamiltonian

The long-wavelength polar LO-phonons are described by the dispersive continuum theory of [7]. It is convenient to work with the reduced ionic displacement field $\boldsymbol{u} = \rho^{1/2}\boldsymbol{w}$ where ρ is the mass density and $\boldsymbol{w}$ the true ionic displacement field. The reduced field satisfies the following vector Helmholtz equation:

$$[\nabla^2 + (\omega_{LO}^2 - \omega^2)\beta^{-2}]\boldsymbol{u} = 0. \tag{1}$$

Here ω_{LO} is the zone-centre LO-phonon frequency and β the acoustic velocity parameter which describes the mode dispersion ($\omega_{LO} = 36.6$ meV and $\beta = 5 \times 10^3$ m s^{-1} for GaAs).

It is convenient to express the solution to (1) in the region $-L/2 < z < L/2$ in the form

$$u_r = (a_r\, e^{iq_z(z-L/2)} + b_r\, e^{-iq_z(z-L/2)})\, e^{i(\boldsymbol{q}_r\cdot r - \omega t)} \tag{2}$$

$$u_z = (a_z\, e^{iq_z(z-L/2)} + b_z\, e^{-iq_z(z-L/2)})\, e^{i(\boldsymbol{q}_r\cdot r - \omega t)} \tag{3}$$

where $\boldsymbol{q}_r$ and $\boldsymbol{q}_z$ are the wavevectors along and perpendicular to the interfaces respectively, with a and b mode amplitudes. The dispersion relation is obtained by applying the appropriate boundary condition at the interfaces. Within the spirit of the hydrodynamic theory, the correct boundary condition for a free-standing slab is simply the vanishing of the pressure (i.e. $\nabla \cdot \boldsymbol{u} = 0$) at the interfaces. This leads, together with the requirement

that the modes are purely longitudinal (i.e. $\nabla \times \boldsymbol{u} = 0$), to standing modes. The normal wavevector is quantised as expected, viz:

$$q_z = m\pi/L \qquad m = 1, 2, 3 \ldots \tag{4}$$

with the field components given by (emitting the common exponential factor)

$$u_r = 2\mathrm{i}\, a_r \sin[q_z(z - L/2)] \tag{5}$$

$$u_z = 2(q_z/q_r)a_r \cos[q_z(z - L/2)]. \tag{6}$$

The resulting dispersion relation simply turns out to be

$$\omega^2 = \omega_{\mathrm{LO}}^2 - \beta^2 Q^2 \tag{7}$$

where $\boldsymbol{Q} = (\boldsymbol{q}_r, \boldsymbol{q}_z)$. It follows from (7) that the number of modes, m, for a given wafer of width L is just

$$m = \mathrm{Int}(\omega_{\mathrm{LO}} L/\beta\pi) \tag{8}$$

where Int(. . . .) designates the integer part of (. . .). Although there are a number of modes for a given practical width we will see that only the lowest order modes are of any significance regarding the electron–phonon interaction with the $m = 1$ mode the most dominant. It should be noted that u_z is non-zero at the interfaces.

The next step is to determine the interaction Hamiltonian. This is achieved by relating the total energy in the cavity to that of an equivalent harmonic oscillator [9]:

$$\frac{1}{2}\frac{\bar{M}}{V_0}\omega^2 \int_V \boldsymbol{w}^* \cdot \boldsymbol{w}\, \mathrm{d}V = \tfrac{1}{2}\bar{M}\omega^2 X_Q^2. \tag{9}$$

The above determines the coefficient a_r and together with the relationship between the mode potential Φ and the ionic displacement $\boldsymbol{w}$

$$\nabla\Phi = (e^*/V_0\varepsilon_0)\boldsymbol{w} \tag{10}$$

leads to the following interaction Hamiltonian

$$\hat{H}_{\mathrm{int}} = -e\Phi = -\mathrm{i}\left(\frac{2}{N}\right)^{1/2} \frac{ee^*}{\varepsilon_0 V_0} \sum_{q_r, q_z} \left(\frac{1}{Q}\sin[q_z(z - L/2)]\, \mathrm{e}^{\mathrm{i}q_r \cdot r} X_Q + \mathrm{cc}\right). \tag{11}$$

In the above e^* is the Callen effective charge, V_0 the volume of the unit cell, N the number of unit cells in the cavity and X_Q the coordinate of the harmonic oscillator. The interaction has the correct Fröhlich form being inversely proportional to the phonon wavevector Q.

It should be pointed out that there are no interface modes which are purely longitudinal (i.e. $\nabla \times \boldsymbol{u} = 0$). The reason for this is as follows. Interface modes may be obtained by replacing $\boldsymbol{q}_z$ by $\mathrm{i}\boldsymbol{q}_z'$ in the formalism where $\boldsymbol{q}_z'$ is a real wavevector characterising the decay. From the vanishing of the pressure at the boundary this wavevector satisfies $\sinh(q_z' d) = 0$ which leads to $q_z' = 0$ for all modes, this is unphysical since, from (5) and (6), the mode amplitude is identically zero. (Note that for the standing modes the boundary condition led to $\sin q_z d = 0$ and hence the quantisation of the normal wave vector.) Any surface modes that are allowed cannot be described by an $e\Phi$ Fröhlich Hamiltonian which applies only to longitudinal excitations. Surface phonon polaritons which are transverse solutions to Maxwell's equations are allowed, indeed they have been extensively studied [13–15]. Polaritons are coupled photon–transverse-optic-phonon excitations which have an electromagnetic part as well as a mechanical

component. The mechanical component contributes to the usual deformation potential scattering which in any case does not effect electrons in a Γ minima [16]. The electromagnetic contribution scatters the carriers only very weakly [17] since the correct interaction Hamiltonian is the usual $\boldsymbol{p} \cdot \boldsymbol{A}$ where $\boldsymbol{p}$ is the momentum of the carrier and $\boldsymbol{A}$ the transverse vector potential associated with the polariton. Some confusion over this point has occurred in the literature; e.g. [18, 19]. In the so-called non-retarded limit $(\omega^2\varepsilon(\omega)/c^2 \to 0)$ where $\varepsilon(\omega)$ is the frequency dependent dielectric function and c the velocity of light in vacuo, the transverse vector potential $\boldsymbol{A}$ may be expressed, in this limit, as the gradient of a scalar function φ (i.e. $\boldsymbol{A} = \nabla\varphi$). The modes have then been coupled to the electrons assuming a Fröhlich type of interaction, $e\varphi$, leading to an exaggerated scattering rate. The correct coupling should be $\boldsymbol{p} \cdot \nabla\varphi$ and calculations are at present under way to determine the electron–polariton scattering rates [20].

3. The scattering rate

We are now in a position to couple these modes to the electrons. It is often the case in transport studies that we are interested in the extreme quantum limit in which only the lowest subband is of importance. Here we only deal with this case although the generalisation to intersubband events is straightforward.

Within the effective mass and parabolic band approximation the normalised electron wavefunctions are of the form

$$\Psi(\boldsymbol{r}, z) = A^{-1/2}\, \mathrm{e}^{\mathrm{i}\boldsymbol{k}\cdot\boldsymbol{r}}\, \psi_{(i)}(z) \tag{12}$$

with corresponding energy

$$E = E_k + E_{(i)} \tag{13}$$

where $E_k = \hbar^2k^2/2m^*$ and $E_{(i)}$ the subband energy. In the above A is the area of the slab, $\boldsymbol{k}$ the wavevector in the plane and m^* the effective mass. The envelope function $\psi_{(i)}(z)$ and subband energy $E_{(i)}$ depend on the choice of confining potential. We consider two types of potential, the often used infinite square well and the more realistic harmonic oscillator potential.

The simplest confining potential is that of an infinite square well of width d. The envelope function for the lowest subband is then

$$\psi_{(1)}(z) = (2/d)^{1/2} \cos(\pi z/d) \tag{14}$$

with corresponding subband energy

$$E_{(1)} = \hbar^2\pi^2/2m^*d^2. \tag{15}$$

On the other hand, the harmonic oscillator confining potential (of frequency Ω) has the following subband wave function

$$\psi_{(2)}(z) = \pi^{-1/4} z_0^{-1/2}\, \mathrm{e}^{-z^2/2z_0^2} \tag{16}$$

with $z_0 = (\hbar/m^*\Omega)^{1/2}$ and subband energy

$$E_{(2)} = \tfrac{1}{2}\hbar\Omega. \tag{17}$$

In order to compare the two situations we take the width of the electron density for the quadratic potential $\psi^*_{(2)}(z)\psi_{(2)}(z)$, to coincide with d the width of the square well (i.e.

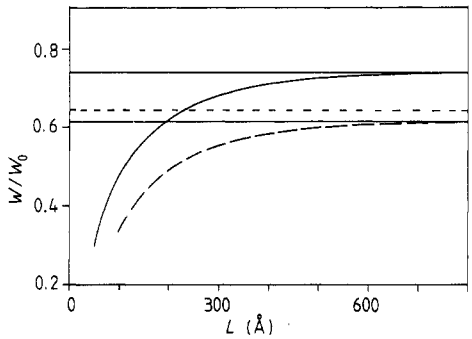

Figure 2. The scattering rate as a function of slab thickness. The full curve illustrates the result obtained from an infinite confining potential whilst the broken curve that obtained assuming a harmonic potential. The full horizontal lines show the appropriate limiting values whilst the broken line is the bulk result [16].

$z_0 = 1/2d$). The Gaussian wavefunction $\psi_{(2)}(z)$ will only be a good representation if $L \gg z_0$ which for a width $d = 50$ Å will easily be the case in practice, otherwise a variational wave function is required.

The scattering rate is given by Fermi's golden rule

$$W = \frac{2\pi}{\hbar} \int |\langle \mathrm{f}|\hat{H}_{\mathrm{int}}|\mathrm{i}\rangle|^2 \delta(E_\mathrm{f} - E_\mathrm{i})\, \mathrm{d}S_\mathrm{f} \tag{18}$$

where i (f) stands for the initial (final) state and the integral is over all final states. The integration is straightforward and we find for the infinite square well

$$W = 8\pi^2 W_0 \left(\frac{\hbar\omega_{\mathrm{LO}}}{E_{(1)}}\right)^{1/2} \alpha \sum_{Q_z} \frac{|G(Q_z)|^2}{\{Q_0^4 + 2(2K^2 - Q_0^2)Q_z^2 + Q_z^4\}^{1/2}} \tag{19}$$

with $\alpha = d/L$, $Q_z = q_z d$, $K = kd$, and $Q_0 = (2m^*\omega_{\mathrm{LO}}/\hbar)^{1/2} d$. The characteristic rate W_0 is given by

$$W_0 = (e^2/4\pi\hbar)(2m^*\omega_{\mathrm{LO}}/\hbar)^{1/2}(1/\varepsilon_\infty - 1/\varepsilon_\mathrm{s}) \tag{20}$$

with ε_∞ and ε_s the high and low frequency dielectric permittivities; for GaAs $W_0 \sim 7.7 \times 10^{12}\ \mathrm{s}^{-1}$. The function $G(Q_z)$ arises from the matrix element and is given by

$$G(Q_z) = -\tfrac{1}{2}\sin\left(\frac{m\pi}{2}\right) \frac{\sin(Q_z/2)}{(Q_z/2)} \left(\frac{\pi^2}{\pi^2 - (Q_z/2)^2}\right). \tag{21}$$

This is equivalent to the integral one obtains for Q2D electrons interacting with bulk polar LO modes [3]. Note that (21) picks out only modes with odd m and the sum in (19) is over all these modes consistent with (8). The corresponding scattering rate for a harmonic potential is simply given by (19) but with $G(Q_z)$ replaced by $\tilde{G}(Q_z)$ where

$$\tilde{G}(Q_z) = -\tfrac{1}{2}\sin(m\pi/2)\, \mathrm{e}^{-Q_z^2\gamma^2/4} \tag{22}$$

and $\gamma = z_0/d$. As with the infinite square well, only phonons having odd index m contribute to the rate.

Figure 2 illustrates the variation of the scattering rates as a function of slab thickness L. In both cases the electrons are confined to a sheet of width $d = 50$ Å with a fixed

carrier in-plane kinetic energy, $E_k = 5\hbar\omega_{LO}$ chosen. Qualitively both curves show the same features. For large wafer thicknesses they are asymptotic to the value obtained when the polar modes are simply bulk plane waves as indeed they should. For widths less than about 500 Å the effects of phonon confinement manifest themselves and we find a marked reduction in the rate for small slab thickness. Similar behaviour is predicted for the corresponding Q1D system [21]. (The curve corresponding to the quadratic potential terminates at $L = 100$ Å as we require $L \gg 25$ Å). It should be noted that the rate at $L = 50$ Å is consistent with the results of Riddoch and Ridley [19] although their rates for interface mode scattering (which are comparable to the standing mode rates) are overestimated due to the reasons outlined in the previous section. It is also predicted that the effect of a harmonic confining potential is to reduce the scattering rate (as compared to the infinite case) by around 17%. This is primarily due to the difference in subband energies and the penetration of the electron wavefunction outside the region $-d/2 \leqslant z \leqslant d/2$. Similar results are obtained in other calculations in which the carriers ae not strictly confined to a given region; e.g. [22]. The overall behaviour is, however, unaffected at least in the extreme quantum limit where we are dealing with intrasubband events. The situation may not be as straightforward for thicker confining regions where more than one subband is occupied since for a harmonic potential the subband separations are equal whereas for the infinite square well they are not. We do not dwell on these complications here.

4. Conclusion

We set out in this investigation to look at the electron–polar-LO-phonon interaction in novel thin free-standing GaAs wafers. Our aim was twofold. Firstly to determine the film thicknes that is needed to observe confined phonon effects in the scattering rate. For typical electron energies we find that film thicknesses less than about 500 Å are required to observe deviations from bulk 3D phonon behaviour. As for scattering via interface modes, we have argued that employing a physically intuitive boundary condition no purely longitudinal surface modes are allowed. Surface phonon polaritons are, of course, normal modes of the system and a qualitative argument was outlined to show that their interaction with electrons ought to be weak (as compared to the LO standing waves). This is not believed to be the case in the $GaAs/Al_xGa_{1-x}As$ system ($x \leqslant 0.3$) in which purely longitudinal interface modes are predicted to exist and are mainly responsible for relaxing the carrier energy at high temperatures, especially for narrow wells [9]. This makes the prospect of fabricating high mobility devices with these free-standing structures promising, although the fabrication technology is still in its infancy. The details of the electron–polariton scattering needs to be quantified and work is underway in this direction. Secondly the effect of a more realistic harmonic confining potential was considered. Although the qualitative behaviour is unaffected, the rate associated with a quadratic confining potential is found to be about 17% less than that associated with the infinite well. It is interesting to note that for the parameters chosen the rate associated with the harmonic oscillator potential lies below the well-known scattering rate for bulk 3D electrons emitting bulk 3D phonons.

Acknowledgments

We thank Dr M Babiker for useful discussions, and one of the referees for insisting on the clarification of some points in this paper. One of us (NCC) thanks the UK Science and Engineering Research Council for financial support.

References

[1] Price P J 1981 *Ann. Phys., NY* **133** 217
[2] Ridley B K 1982 *J. Phys. C: Solid State Phys.* **15** 5899
[3] Leburton J P 1984 *J. Appl. Phys.* **56** 2850
[4] Klein M V 1986 *IEEE J. Quantum Electron.* **QE-22** 1760
[5] Jain J K and Das Sarma S 1989 *Phys. Rev. Lett.* **62** 2305
[6] Dharssi I and Butcher P N 1990 *J. Phys.: Condens. Matter* **2** 119
[7] Babiker M 1986 *J. Phys. C: Solid State Phys.* **19** 683
[8] Babiker M and Ridley B K 1986 *Superlatt. Microstruct.* **2** 287
[9] Ridley B K 1989 *Phys. Rev.* B **39** 5282
[10] Tatham M C, Ryan J F and Foxon C T 1989 *Phys. Rev. Lett.* **63** 1637
[11] Hasko D G, Potts A, Cleaver J R A, Smith C G and Ahmed H 1988 *J. Vac. Sci. Technol.* **6** 1849
[12] Kelley M J private communication
[13] Kliewer K L and Fuchs R 1966 *Phys. Rev.* **144** 495
[14] Boardman A D (ed) 1982 *Electromagnetic Surface Modes* (New York: Wiley) ch 6
[15] Cottam M G and Tilley D R 1989 *Introduction to Surface and Superlattice Excitations* (Cambridge: Cambridge University Press) ch 6
[16] Ridley B K 1982 *Quantum Processes in Semiconductors* 2nd edn (Oxford: Oxford University Press)
[17] Chamberlain M P and Babiker M 1989 *J. Phys.: Condens. Matter* **1** 1181
[18] Ridley B K 1985 *Festkörperprobleme (Advances in Solid State Physics)* vol 25 (Braunschweig: Vieweg) p 449
[19] Riddoch F A and Ridley B K 1985 *Physica* B **134** 342
[20] Al-Dossary, Babiker M and Constantinou N C 1990 unpublished
[21] Constantinou N C and Ridley B K 1990 *Phys. Rev.* B **41** 10622
[22] Constantinou N C and Ridley B K 1989 *J. Phys.: Condens. Matter* **1** 2283